HYSTORE

Hybrid Services from Advanced Thermal Energy Storage Systems

D2.3 – Report on the selection of TCM materials for solution IV and the characterization

1. Table of Contents

2. List of Figures

3. List of Tables

PROJECT DURATION: 1 January 2023 – 31 December 2026
GRANT AGREEMENT ID: 1010967 (Innovation Action)
WP: 2 **DELIVERABLE:** 2.3
LEAD BENEFICIARY: CNR
SUBMISSION DATE: 17 September 2023
DISSEMINATION LEVEL: Public
DUE DATE: M9
HYSTORE Website: https://www.hystore-project.eu/
REVISION HISTORY:

DATE	VERSION	AUTHOR/CONTRIBUTOR	REVISION BY	COMMENTS
25/07/2023	0.0	CNR		
22/08/2023	0.1	INOVA		
28/08/2023	1.0		CNR	
06/09/2023	2.0		CNR	
06/09/2023	2.1		ARC	
18/09/2023	2.2		AIT	
18/09/2023	3		CNR, INOVA	

DISCLAIMER

ACKNOWLEDGEMENT

This project has received funding from the European Union's Horizon Europe research and innovation programme under grant agreement Nº 1010967.

Funded by the European Union

"Funded by the European Union. Views and opinions expressed are however those of the author(s) only and do not necessarily reflect those of the European Union or European Climate, Infrastructure and Environment Executive Agency (CINEA). Neither the European Union nor the granting authority can be held responsible for them.."

4. Executive Summary

HYSTORE project aims at developing different thermal energy storage solutions that would not only serve as a means for improving the energy efficiency of the buildings where they will be installed, but also as an asset to the electric grid. One of the solutions for storing heat for a period of up to 4 weeks is the use of a thermochemical energy storage. The goal of this report is to present the selection of the material to be used within the thermochemical HYSTORE solution. To this aim, a decision process based on a weighted scoring system was used, which takes into account both technical and economic constraints. The methodology consists of 5 steps:

1. Literature Review
2. Criteria Selection
3. Weighting of Criteria
4. Scoring System
5. Evaluation and Ranking

Out of this process, the zeolite 13X produced in Italy by UOP was selected and a characterization campaign was carried out. This consisted of both thermo-physical characterization (adsorption capacity, specific heat) and thermo-electrical characterization (i.e. measurement on the impedance of the material and drying time under RF heating). The latter, takes into account the operating conditions of HYSTORE, which consist of charging using radio-frequency. Finally, the discharging behaviour was addressed by means of a validated model developed in COMSOL Multiphysics.

The authors of the report are: Valeria Palomba (CNR), Cristina Santoloce (INOVA), Chiara De Massari (INOVA), Vanessa Garcia (INOVA). The contributors to the report are Girolama Airò Farulla (CNR), Vincenza Brancato (CNR), Andrea Frazzica (CNR), Gabriele Penello (SOR).

5. Introduction

5.1. Summary

Thermochemical energy storage (TCES) systems have emerged as promising technologies for efficient and sustainable energy storage. The selection of suitable materials plays a critical role in the design and performance of TCES systems. This report outlines a comprehensive selection procedure that utilizes scientific literature and a set of predetermined criteria to assess and score potential materials for thermochemical energy storage applications.
Thermochemical energy storage involves the use of reversible chemical reactions to store and release heat energy. The selection of materials for TCES systems is crucial to ensure high energy storage capacity, stability, and overall system efficiency. To facilitate an effective and informed decision-making process, a systematic approach is proposed, incorporating data from scientific literature and criteria-based assessment. The results led to the selection of the final candidate for the thermochemical material (TCM) storage for the HYSTORE TCM prototype.

5.2. Relation to other activities

The characterization here reported has been carried out within the activities of T2.3. The results will be fed to T2.4 (Heat Exchanger, HEX, design) and to WP3 for the design and development of the storage system as a whole (material, reactor and auxiliaries) and are obtained through simulations and experimental activities in lab-scale. Moreover, the selection criteria used are based also on the performance indicators and use cases identified in WP1.

5.3. Contribution of partners

CNR is task responsible and main editor of the report. INOVA contributed to the deliverable by realising characterization of the selected material under HYSTORE operating conditions for the TCM (charging through radiofrequency devices, RF). SOR, as manufacturer of the storage and industrial partner, contributed with CNR to the definition of the selection criteria and their weight.

5.4. Structure of the deliverable

The deliverable is structured as follows:

- Section 6 describes the selection procedure and final choice of? the thermochemical material for HYSTORE;
- Section 7 presents the main thermophysical characterization carried out at CNR;
- Section 8 presents the thermo-electrical characterization carried out at INOVA under charging conditions;

- Section 9 presents a preliminary model of the material to evaluate the discharging behaviour;
- Section 10 contains the conclusions.

6. Identification of TCM materials

6.1. Methodology

The methodology followed is described below. It consists of 5 steps:

1. Literature Review:

The first step involves an extensive review of the scientific literature to identify potential materials suitable for TCES applications. The literature review encompasses studies, research articles, and patents related to TCES, focusing on materials with desirable thermodynamic properties, reaction kinetics, and thermal stability.

2. Criteria Selection:

A set of criteria is established to evaluate and compare the identified materials. The criteria should be based on key performance indicators and properties relevant to TCES systems. Examples of criteria include energy storage capacity, reaction kinetics, thermal stability, abundance, cost, scalability, and environmental impact.

3. Weighting of Criteria:

Each criterion is assigned a weight that reflects its relative importance in the material selection process. The specific criteria and weights used in the selection procedure vary depending on the objectives and constraints of the TCES system. It is important to customize the criteria and weights according to the specific needs of the project.

4. Scoring System:

A scoring system is developed to assess each material against the selected criteria. A numerical scale, such as 1 to 10, will be employed, with higher scores indicating better performance. The scoring will be based on experimental data, theoretical predictions, commercial data etc…

5. Evaluation and Ranking:

Using the assigned weights and scores, a comprehensive evaluation is conducted for each material. The scores for each criterion are multiplied by their corresponding weights and summed to obtain a weighted score for each material. The materials are then ranked based on their weighted scores, with higher-ranking materials being more suitable for the specific application.

6.2. List of materials and their properties

Sorption storage materials

The most common adsorbent materials for adsorption reactions are: zeolites [1] [2], zeotypes [3] [4], silica gels [5] [6] and Metal-Organic Frameworks (MOFs) [7] [8].

Zeolites are crystalline aluminosilicate adsorbents with a microporous structure and are frequently referred to as "molecular sieves". Their structural foundation is a combination of SiO_4 and AlO_4 tetrahedra that are linked by oxygen atoms to create an open crystalline structure with micropores that can serve as hosts for molecules. There are presently 232 zeolites that can be identified based on the type of framework.

This suggests that there is a wide range in both the composition and the characteristics of zeolites, especially based on the cations and anions in their structure.

Zeotype are materials, such as Silicoaluminophophate (SAPOs) and Aluminophophate (AlPOs), with a regular crystalline structure and a consistent porosity structure. These substances differ from zeolites in that they have a neutral framework, which means that extra-framework cations are absent. Some zeotypes exhibit extremely high water adsorption capacities despite the absence of cations, which should cause them to behave hydrophobically. In addition, ALPOs are characterized by a water adsorption isotherm V, which makes them particularly appealing for TES applications because of their ability to regenerate in a limited temperature range. However, their application is limited by the high cost and low availability.

A family of porous physical sorbents that have been extensively explored for use in water adsorption applications are silica gels. Unlike zeolites and other traditional sorbents, silica gels are amorphous substances. Different silica gels have been manufactured and tried so far for medium to long term Thermal Energy Storage (TES) applications because of their capacity as water sorbents. A wide range of porous materials can be produced depending on the synthesis methods, especially as the pore size can be changed from micro to meso-pores, which has a significant impact on the water vapour adsorption capabilities. Silica gels have been viewed as potential for significant TES applications since they are readily available commercially and are reasonably priced. Due to the tiny amount of water vapour exchanged between charging and discharging in long-term TES circumstances, the results showed that the possible storage density is highly constrained.

(MOFs) are the most alluring new class of adsorbents for use in thermally driven sorption systems (i.e., for heating, cooling, and storing). This family of adsorbents is distinguished by inorganic clusters (such as metals) linked to one another by a framework of organic ligands, producing a mono-, bi-, or tri-dimensional porous structure. Wide specific surface area (up to 4000 m^2/g) and wide specific pore volume (up to 1.14 cm^3/g) are two characteristics of this structure that make it a promising water vapour adsorbent. Since there are practically endless combinations of inorganic clusters and organic ligands, around 20,000 distinct MOFs have so far been created. This means that, on the one hand, there is the interesting possibility of tailoring the adsorbent to the specific application. On the other, however, activity on MOFs for TES applications is still at lab-level, with many efforts dedicated towards the development of more stable and inexpensive materials.

Another possible material choice is the one of composite materials, obtained by impregnation of the salts into porous matrix. Recently, the research activity on this class of materials is booming since they probably represent the most attractive solution towards the application of sorption TES for solar thermal energy ([9]). The most investigated porous matrixes are zeolites, silica gels, clays and carbonaceous materials.

6.3. Criteria selection

The parameters that represent the list of criteria for the final selection of TCM were chosen because of their direct impact on the storage from the operational and economic points of view, considering also the list of Key Performance Indicators (KPIs) selected in WP1. The following ones were chosen:

- Energy storage capacity: The ability of the material to store and release heat energy efficiently.
- Reaction kinetics: The rate at which the reversible chemical reaction occurs, affecting the charging and discharging times of the system.
- Thermal stability: The ability of the material to withstand repeated thermal cycling without significant degradation.
- Abundance: The availability and accessibility of the material on a large scale.
- Cost: The economic feasibility of using the material for TCES systems, including production costs and material availability.
- Scalability: The potential for large-scale implementation.

As discussed above, each criterion was associated with a % weight, in order to derive the final scoring of materials. The weight selection considers the specific TRL (i.e up to 6) and use cases of the project, therefore higher weights were associated to cost and availability of the various materials.

The list of criteria and weights is shown in **Error! Reference source not found.**. The overall sum of % weights is 100%.

Table 1 weights associated to selected criteria for materials' scoring.

Criterion	% weight
Energy storage capacity	35
Reaction kinetics	10
Thermal stability	10
Abundance and Cost	35
Scalability	10

6.4. Materials pre-selection

The materials pre-selected for the evaluation belong to the classes presented in the previous section. More in detail, materials representative of the features of each class were selected, for which experimental characterization on the heat storage capacity was available from internal CNR database of measurements.

The following materials are discussed in the following:

- Synthetic zeolites FAM Z01 and FAM Z02. They are produced by Mitsubishi chemicals[1] and have been widely discussed in the literature as water sorbents.
- Silica gels commercially produced by Fuji Chemical Industries and OkerChemie.

[1] See the following sections for the more updated information on their availability

- DDZ-70, a zeolite commercialised by UOP, which is a high silica content Y zeolite exchanged with cerium to reduce its hydrophilicity;
- 13X zeolite produced by UOP, which is a highly selective molecular sieve widely used in the oil and gas industry;
- Zeolite Y commercialised by Sigma Aldrich.
- A composite realised by wet impregnation of silica gel with calcium chloride, realised internally at CNR ITAE using the methodology discussed in [10].

Storage capacity

A first pre-selection of candidates was carried out considering only the storage capacity of the material. The storage capacity can be calculated (heat storage use case) as:

$$E_{heating} = \Delta H_{ads} \Delta w \quad (1)$$

Where $E_{heating}$ is the specific energy (in kJ/kg) that the material can store considering heating conditions, ΔH_{ads} is the adsorption enthalpy (kJ/kg) and Δw is the amount of refrigerant exchanged during the process.
For the application as cold storage, the storage capacity can be calculated as:

$$E_{cooling} = \Delta H_{evap} \Delta w \quad (2)$$

Where $E_{cooling}$ is the specific energy (in kJ/kg) that the material can store considering heating conditions, ΔH_{evap} is the evaporation enthalpy of the refrigerant (kJ/kg) and Δw is the amount of refrigerant exchanged during the process.
To evaluate the storage capacity of the different materials, the equilibrium curves of the various materials can be used, since from them it is possible to evaluate both terms from equations (1) and (2). The procedure used to calculate the enthalpy of adsorption from isobars of the material is described in detail in [11]. All the measurements were done at CNR using either a Cahn microbalance or a modified TG/DSC equipment with dedicated water vapour line. The heat of adsorption is a function of the loading w. However, for evaluation's sake, the average value between the adsorption enthalpy at the minimum loading w_{min} and the maximum loading w_{max} is considered for each material.
In order to evaluate the operating boundaries for the calculation of the desired parameters, the following assumptions were used:

- Heating use case: condenser pressure of 39 mbar (corresponding to a water saturation temperature of 29°C). Charge temperature: 140°C.
- Cooling use case: evaporator pressure of 12 mbar (corresponding to a water saturation temperature of 10°C). Charge temperature: 140°C.

The isobars for the selected materials at these two pressure levels are reported in Figure 1 for the heating case and in Figure 2 for the cooling case, where the boundaries in terms of charge and discharge temperature are also indicated. For each material, the Δw can be calculated as the difference between the uptake at discharge and the uptake at charge temperature.

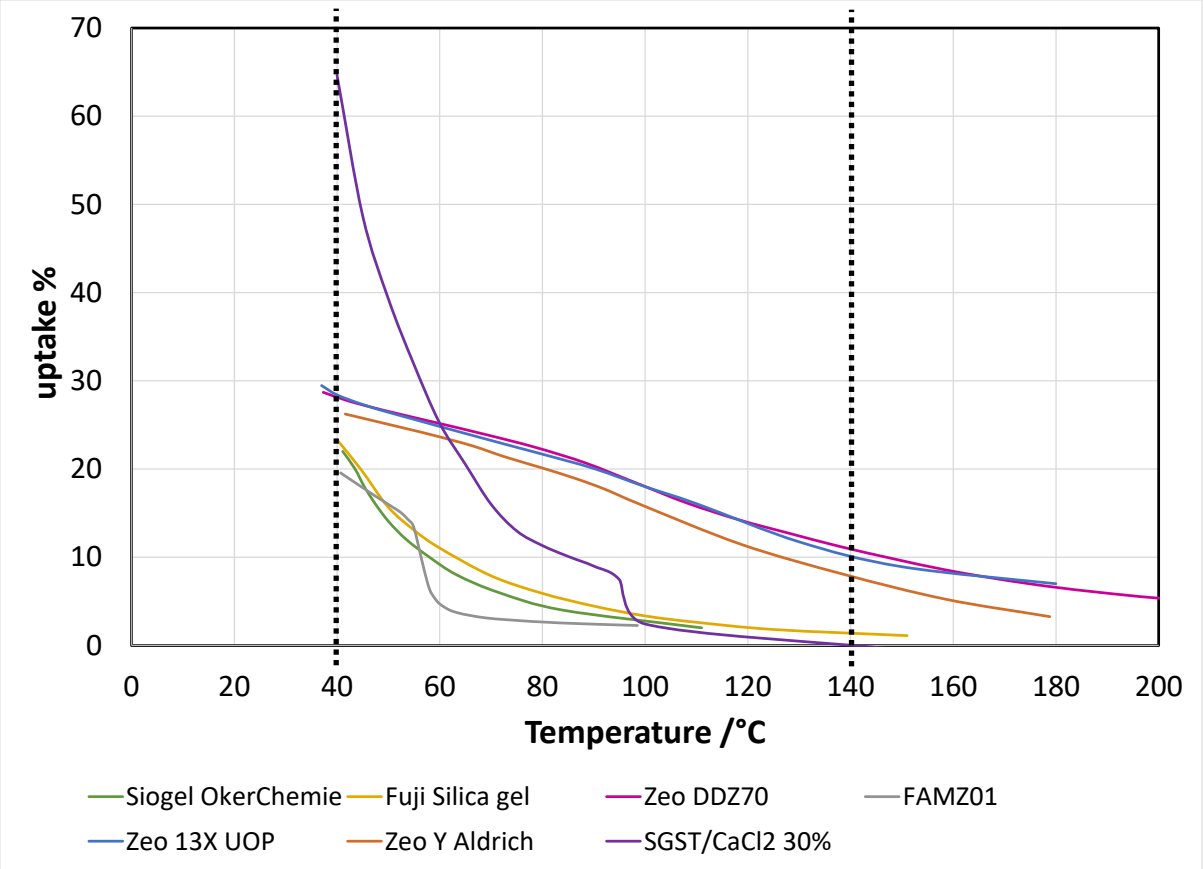

Figure 1: isobars measured experimentally for different materials - heating use case.

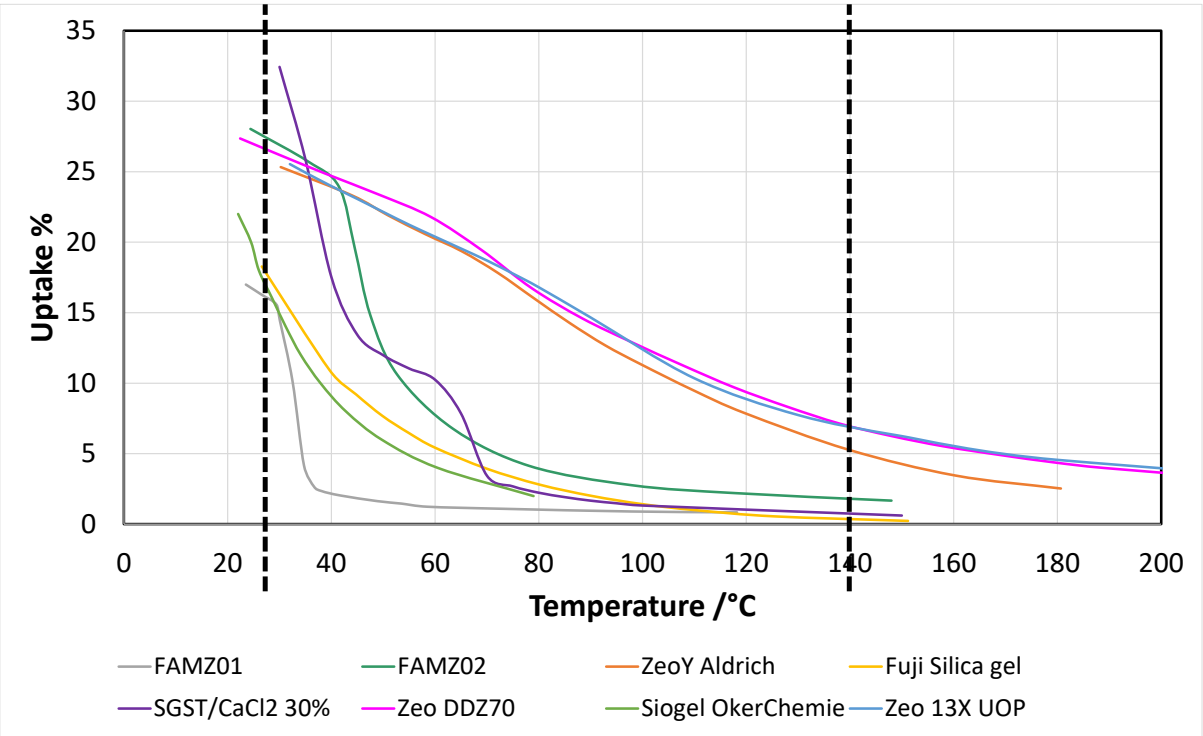

Figure 2: isobars measured experimentally for different materials - cooling use case.

For the materials presented in Figure 1 and Figure 2, the associated adsorption and evaporation enthalpy, the uptake change during the cycle and the theoretical energy storage density are presented in Table 2.

Table 2: energy storage capacity for the list of pre-selected materials.

Material	Heating use case			Cooling use case		
	ΔH_{ads} (kJ/kg_{water})	Δw (%)	$E_{heating}$	ΔH_{evap} (kJ/kg_{water})	Δw (%)	$E_{cooling}$ (kJ/kg)
FAM Z01	3700	20	240	2500	15	375
FAM Z02	4030	22	890	2500	26	650
Zeolite Y Sigma Aldrich	3750	20	750	2500	20	500
Zeo DDZ70	3750	20	750	2500	22	550
Zeolite 13X UOP	3400	20	680	2500	18	450
Fuji Silica gel	2400	20	460	2500	18	450
Oker Chemie Siogel(R)	2400	19	456	2500	18	450
composite SG/CaCl2 30%	1600	65	1040	2500	30	750

6.5. Materials scoring

Starting from the classes of materials presented above, each material was associated with a score (1 to 20) for each of the selected criteria. The reasoning of each score is discussed in the following. The scores are presented in Table 3.

Table 3: scores assigned to each material and criterion.

Material	Energy storage capacity	Reaction kinetic	Thermal stability	Abundance and cost	Scalability
FAM Z01	10	12	20	0	0
FAM Z02	18	12	20	0	0
Zeolite Y Sigma Aldrich	17	14	20	10	8
Zeo DDZ70	17	14	20	15	8
Zeolite 13X UOP	15	18	20	20	20
Fuji Silica gel	12	18	20	20	12
Oker Chemie Siogel(R)	12	18	20	20	16
composite SG/CaCl2 30%	20	10	12	10	10

Regarding FAM Z01 and Z02 materials, despite their good storage capacity (especially for FAM Z02), a score of « 0 » was indicated for the abundance and cost and the scalability categories. Indeed, Mitsubishi Chemicals is no longer producing the

materials and, following a recent request from CNR, has indicated that they are not planning to start again FAM materials production soon. The Zeolite Y from Sigma Aldrich and the DDZ70 zeolite have good energy storage capacity and, as well known from the literature, favourable reaction kinetics. They are also cheap (for large batches, <10 €/kg). However, a low score was given for scalability: both materials are only sold as powders. For the HYSTORE application, this makes them not usable. It is theoretically possible to pelletize them but this requires skills, infrastructure and budgets that are not in line with HYSTORE.
Regarding the zeolite 13X, it has quite balanced properties, in terms of storage capacity and reaction kinetics. It is also possible to acquire large batches (i.e. at least 1 ton) from UOP in Italy in pelletised or beads shape for low price (< 7 €/kg). The need for buying large batches is not an issue, since a first estimation shows that for HYSTORE project it might be needed the purchase of more than 1 ton of material.
Regarding the two silica gels, they are penalised by the lower energy storage capacity than the other materials. The "scalability" category was penalised for the Fuji silica gel, due to the need to acquire it outside Europe.
The composite material has the highest energy storage capacity, but there is no possibility to acquire it on the market. The realisation of small batches (up to 150 kg) was carried out at CNR in previous H2020 funded projects, but its selection would penalise the industrialization aspects of a high TRL project such as HYSTORE. At the same time, proof of long-term stability is not available so far from literature studies or internal CNR studies, which has penalised the correspondent score.

6.6. Decision matrix

The scores assigned were weighted according to the choices reported in section 6.5 and an overall score was defined, as presented in Table 4. The final selection indicated the zeolite 13X from UOP as the selected material for the following activities on TCM within HYSTORE. In the next sections, a more detailed characterisation of the material and a preliminary sensitivity analysis regarding the operating conditions in HYSTORE was carried out.

Table 4: decision matrix with weighted scores and the total for the selected TCMs.

Material	Energy storage capacity	Reaction kinetic	Thermal stability	Abundance and cost	Scalability	Overall score
FAM Z01	3.5	1.2	2	0	0	**6.7**
FAM Z02	6.3	1.2	2	0	0	**9.5**
Zeolite Y Sigma Aldrich	5.95	1.4	2	3.5	0.8	**13.65**
Zeo DDZ70	5.95	1.4	2	5.25	0.8	**15.4**

Zeolite 13X UOP	**5.25**	**1.8**	**2**	**7**	**2**	**18.05**
Fuji Silica gel	4.2	1.8	2	7	1.2	**16.2**
Oker Chemie Siogel(R)	4.2	1.8	2	7	1.6	**16.6**
composite SG/CaCl2 30%	7	1	1.2	3.5	1	**13.7**

7. Thermo-physical characterization of selected materials

7.1. Adsorption capacity

The most relevant data needed for adsorbent working pairs used for adsorption heat transformation processes are represented by the sorption equilibrium curves. The adsorption process of an adsorbate over an adsorbent material is bivariat, meaning that the water adsorption uptake depends on two independent variables, namely, the adsorption temperature and the water vapor pressure. The importance of the equilibrium curves was shown in section 6.4: starting from them, the theoretical energy storage capacity in different operating conditions can be derived.
The experimental measurement can be performed at constant temperature (isotherms) or at constant pressure (isobars). They can also be combined to derive the isosteric chart of the material on the Clausius- Clapeyron diagram. The equipment to measure the equilibrium curves of the material can be either a thermogravimetric one or a volumetric one. In thermogravimetric apparatuses, the curve is obtained by measuring the variation of adsorbent material weight during adsorption process. In volumetric apparatuses the pressure variation occurring in a known volume due to the adsorption is monitored and then converted in adsorption capacity by considering water vapor at low absolute pressure as an ideal gas.
For the HYSTORE project, the existing thermogravimetric apparatus available at the CNR ITAE lab was used. As reported in Figure 3, it is a Dynamic Vapor Sorption setup, which can perform characterization under either isothermal or isobaric conditions. It can perform isotherms from room temperature up to 70 °C and isobars under virtually all the vapor pressures up to ambient pressure. Furthermore, it can operate with different working fluids. The detailed description of the operation is reported in [12].

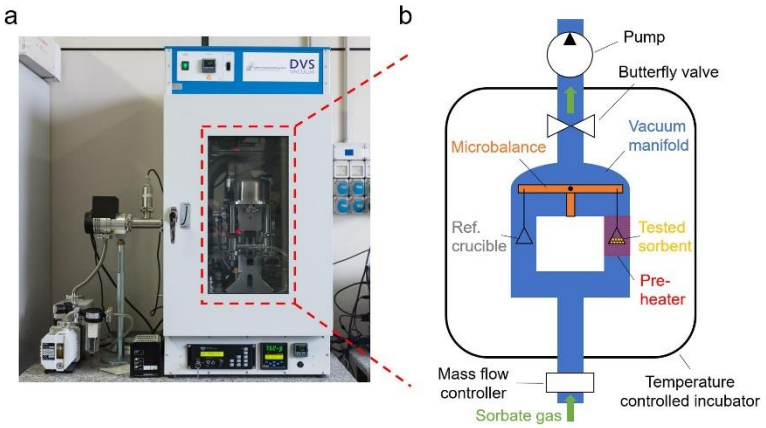

Figure 3: DVS vacuum thermogravimetric apparatus installed in CNR

The isotherm at 30°C is shown in Figure 4. Both an adsorption and desorption run were carried out, to verify the possible presence of hysteresis, which does not occur. The obtained curve was also compared with other existing ones in the literature and a good match was found.

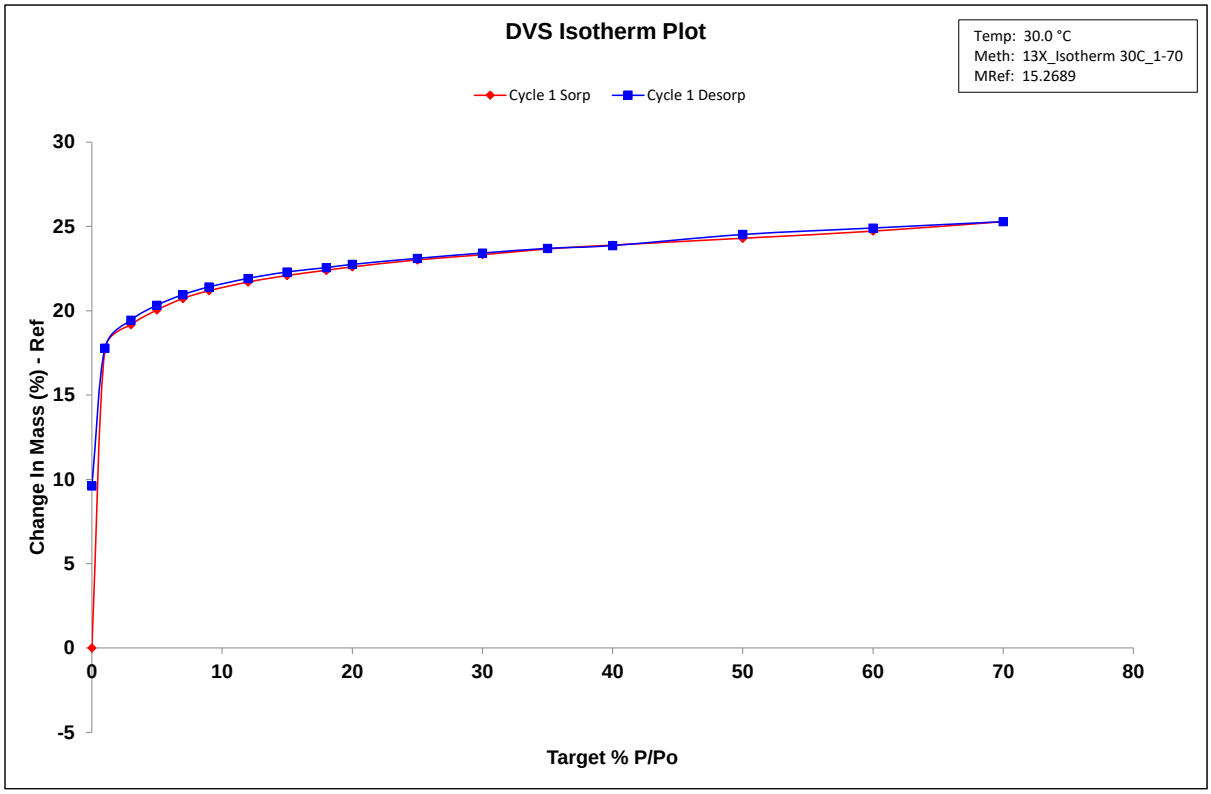

Figure 4: isotherm of UOP 13X at 30°C.

To have more complete information on the material, different tests in isobaric conditions were carried out, whose results are reported in Figure 5. It is possible to notice that all curves have the same trend and they shift towards higher uptakes when the operating pressure is higher.

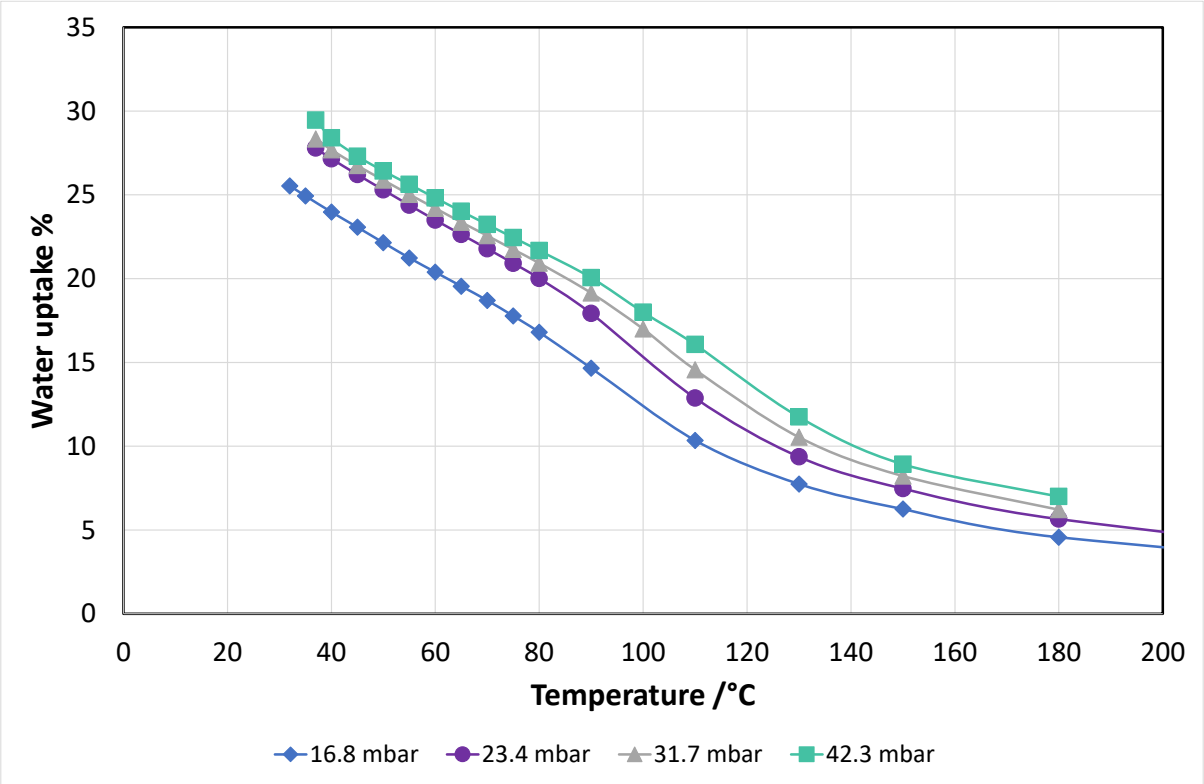

Figure 5: equilibrium curves at different water vapour pressures for zeolite 13X.

The results were further elaborated, to be used within numerical analyses. To this aim, Dubinin-Astakhov approach was used to fit the equilibrium data in order to obtain a temperature independent characteristic curve both for adsorption and for desorption in the following form [13]:

$$W = W_0 \exp\left[-\left(\frac{A}{E}\right)^n\right] \quad (3)$$

where: W (g/g) is the water vapour adsorbed per unit of adsorbent material mass; W0 (g/g) is a maximum water vapour uptake; E (J/g) corresponds to the characteristic energy for the working pair and depends on the sorbent as well as on the adsorbate; A (J/g) is the adsorption potential, defined as follows:

$$A = RT \ln \frac{p_s}{p} \quad (4)$$

in which: R (J/mol K) is the universal gas constant, T (K) the temperature of adsorption or desorption, p_s (kPa) is the saturated vapour pressure at T, p (kPa) is the pressure of the working fluid vapour.

Figure 6 shows the experimental data and the obtained fitting curves for the selected material. The parameters used for fitting the experimental data for all the chosen adsorbent materials are: w0=0.29 g/g; E=869.55 kJ/kg, n=1.56.

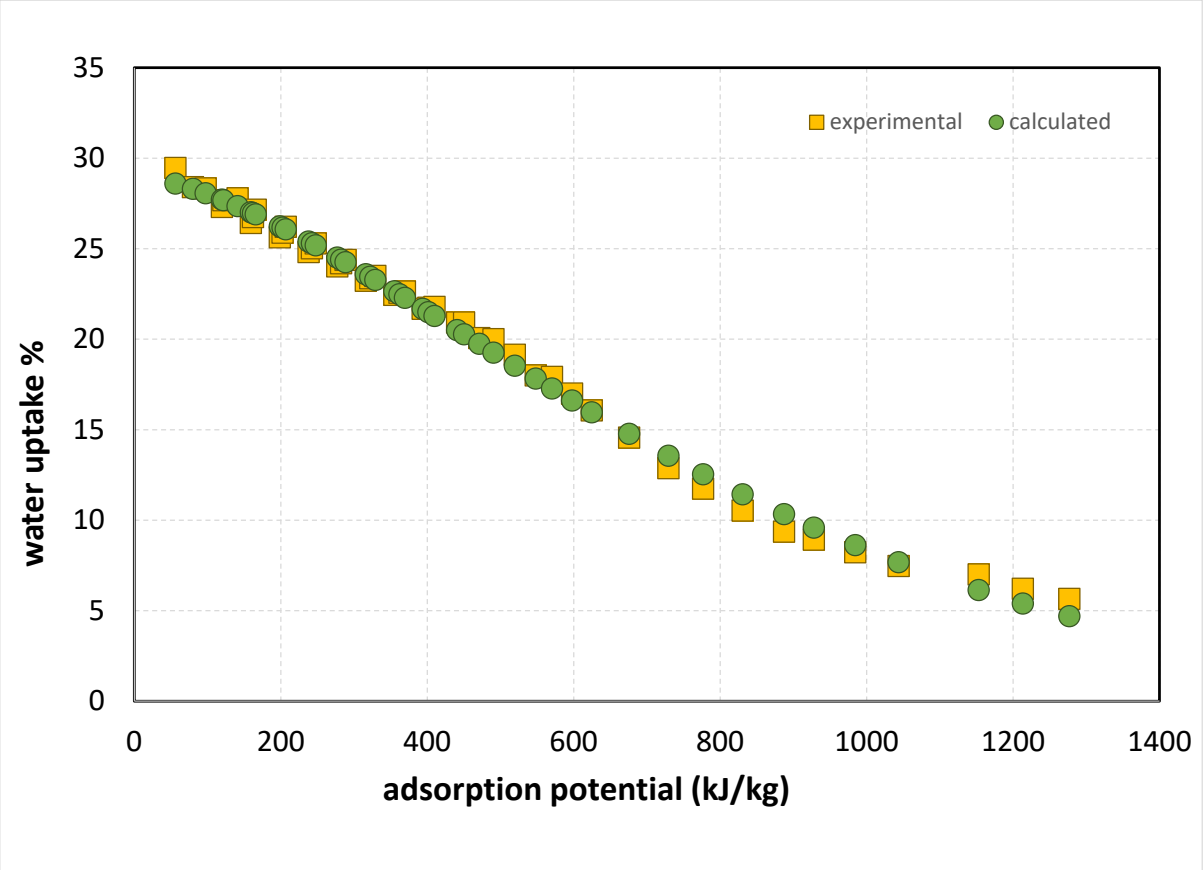

Figure 6: comparison of experimental equilibrium data and the fitted ones according to Dubinin-Ashtakov approach.

7.2. Specific heat

The other thermophysical parameter needed for the evaluation of the storage capacity of a material, and of its dynamic behavior, is the specific heat of the adsorbent material. In order to measure it, a Differential Scanning Calorimeter (DSC) was used. The experimental approach consists in measuring a reference material, in this case alumina, whose specific heat is known and can be used as reference. Afterwards, the unknow sample is measured and the specific heat is evaluated by computing the difference from the heat flux measured on the reference sample. A detailed description of the experimental procedure can be found elsewhere [14].
For the selected adsorbent material, the measurements were performed at the CNR ITAE lab by using a DSC 01 Mettler-Toledo represented in Figure 7. To avoid the influence of adsorbed water vapor over the measurement, the samples were carefully dried in an oven at 150°C for 8 hours and then put inside a crucible and carefully sealed.

Figure 7: DSC 01 Mettler Toledo at CNR ITAE lab.

To compute the effect of adsorbed water, the following equation (5) was used:

$$cp_{ads}(T) = cp_{dry}(T) + cp_{wat}(T)\, w_{ads}(T) \quad (5)$$

It considers that the presence of water increases the specific heat of the adsorbent as a function of the water uptake. In this case, the specific heat of water is considered in its liquid state, which is the most common approach used in the literature. This approach was then used for the thermodynamic calculations. The specific heat obtained is reported in Figure 8.

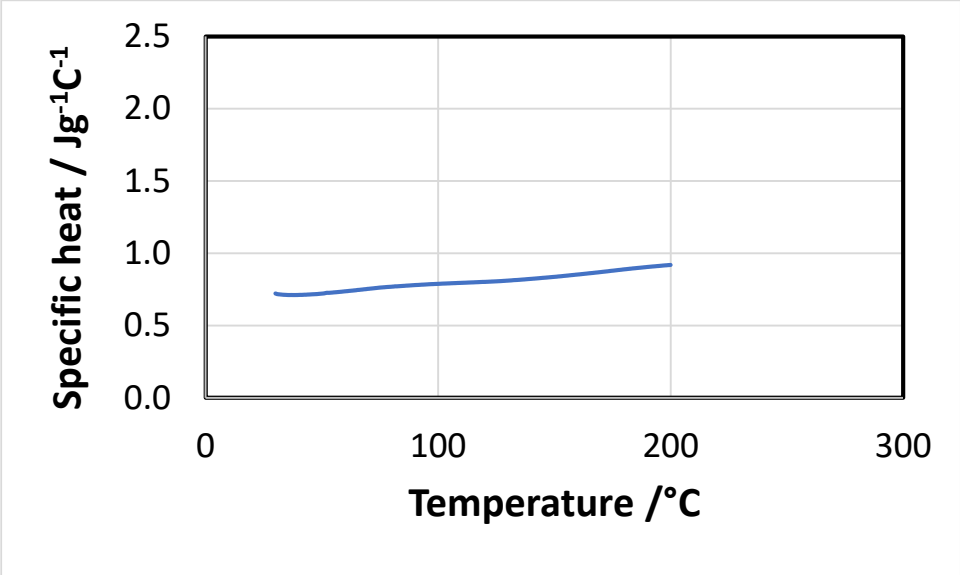

Figure 8: specific heat of UOP 13X

8. Characterization of selected materials under HYSTORE charging conditions

8.1. Equipment description

Following the thermo-physical characterization of the material, another set of tests was carried out at INOVALAB, with the support of CNR and SOR. It takes into account the specific operating conditions of HYSTORE TCM solution, i.e., the direct heating using radio frequency. The list of equipment used for material characterization is as follows:

1. VNA Siglent, Spectrum & Vector Analyzer SVA1000X

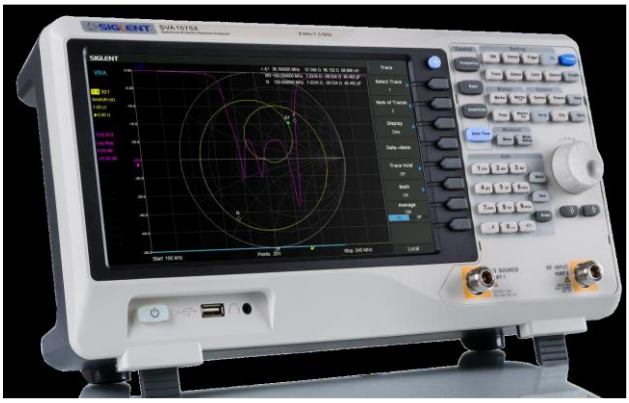

Figure 9: VNA

2. Thermal Camera Flir, FLIR T420
3. Precision Balance Radwag, WLC 2/A2
4. Professional Oven Unox, CHEFTOP XEVC-0711-EPR
5. Radio Frequency Generator Coaxial Power System, RFG 3K-27MHz
   Matching UNIT Coaxial Power System, AMNC
   Matching BOX Coaxial Power System, AMN 3K-27

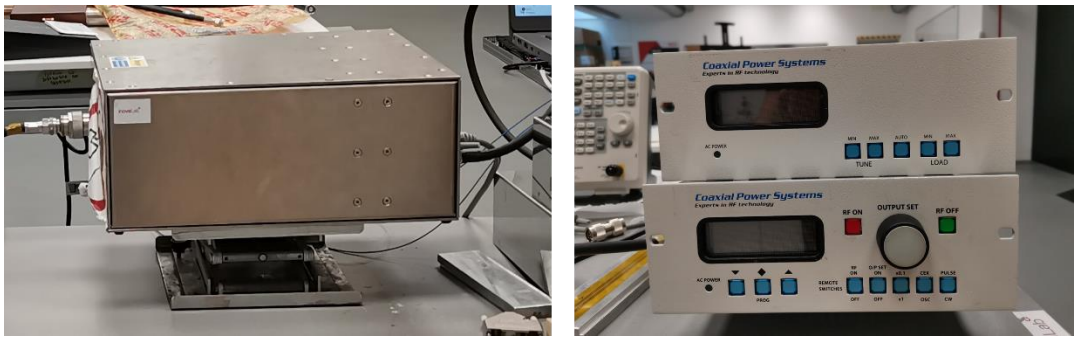

Figure 10: matching box, matching unit, RF generator

6. Optical Fiber Optocon, Fotemp TS3

8.2. Results

8.3. Impedance measurement

Three typologies of 13X material were delivered at Inovalab with dimensions and characteristics listed below. The three samples consist of the same material (the zeolite 13X by UOP described in the previous sections), but differ in the macroscopic arrangements: one sample is made out of pellets, whereas the others are loose grains with different particle size.

Commercial name	Size	Density [lbs/ft^3]	Density [g/cm^3]	Water content as shipped (wt%)	Stability temperature [°C]
13xp 10*20		42	0.672	0.5	400
13xp 8*12		41	0.656	0.5	
13xp (pellets) 1/16"		38	0.608	<1	

Figure 11: Samples of the three materials

Three samples were prepared with similar weight in order to measure their impedance in similar conditions. A Vector Network Analyzer (Instrument 1) was used to perform the impedance measurements at 27.125 MHz, which is the standard industrial frequency used in a wide range of applications.

Before starting the impedance measurements, the samples were dried in order to have the same baseline relative to zero humidity content. The dielectric characteristics of these materials change respect to the inner humidity or moisture level. For this reason, the materials were dried in a professional oven (Instrument 4) at 250°C for 4 hours to reach the 0% humidity level. The materials were weighted in a precision scale (Instrument 3) after the drying treatment; the materials were also weighted precisely after adding the corresponding water level of 10%, 20% and 30% of the weight of the dry sample.

The following Table 5 shows the weight at different humidity levels.

Table 5: weight of the tested samples at different humidity levels.

Sample	Humidity [%]	Weight [g]
10*20	0	212.09
	10	233.30
	20	254.51
	30	275.72
8*12	0	210.98

	10	232.08
	20	253.18
	30	274.27
11/16''	0	206.62
	10	227.28
	20	247.94
	30	268.61

The impedance measurements were performed in a cylindrical metal container with a circular planar electrode. A support was used to maintain a consistent electrode height during the measurements, as showed in the figure below. This ensured a perfect repeatability.

Figure 12: Container and electrode used for the measurement.

The impedance values for each material typology are presented in real and imaginary part in the next graphs.

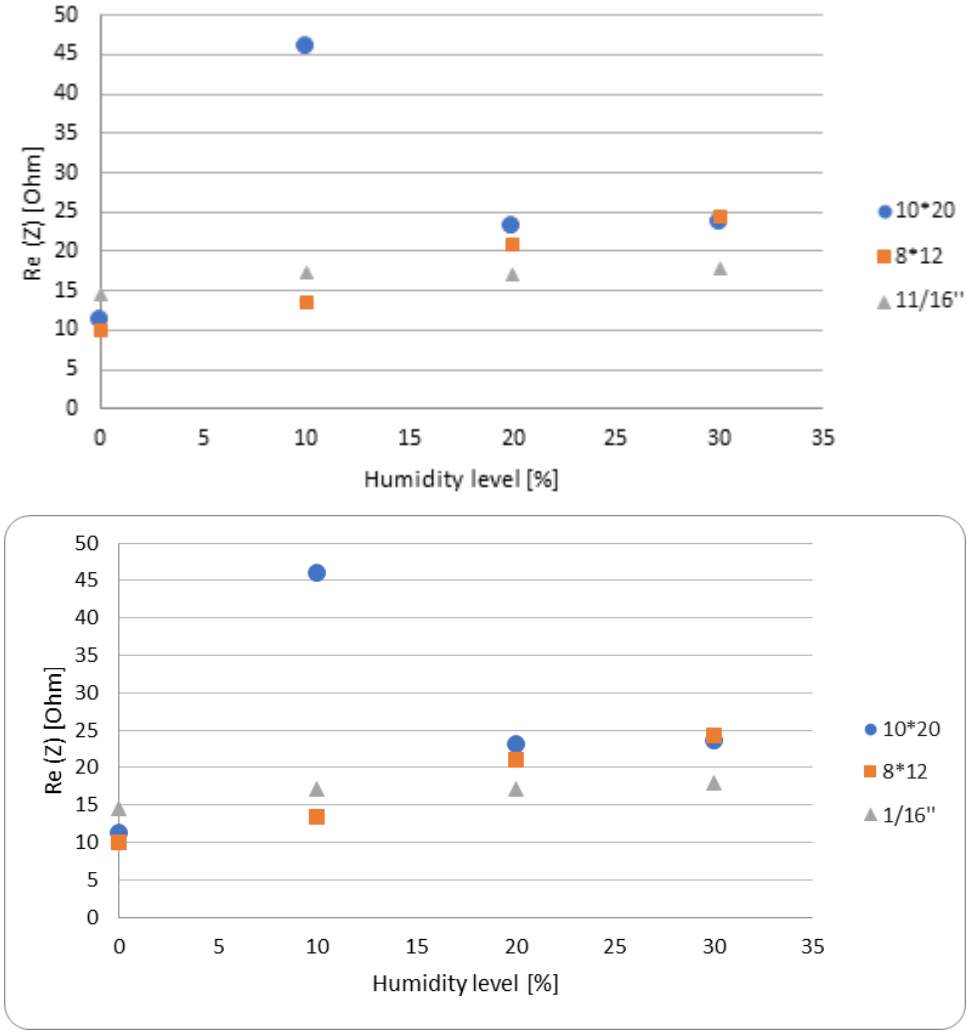

Figure 13: real part of impedance of the tested samples at different humidity levels.

For the impedance real part, a peak of the impedance for the 10x20 material was evident at 10% humidity level. The measurement was repeated exhibiting the same behaviour. As for the 10x20 and 1/16'' materials, a monotonous increasing function of the impedance real part was shown respect to the humidity level.

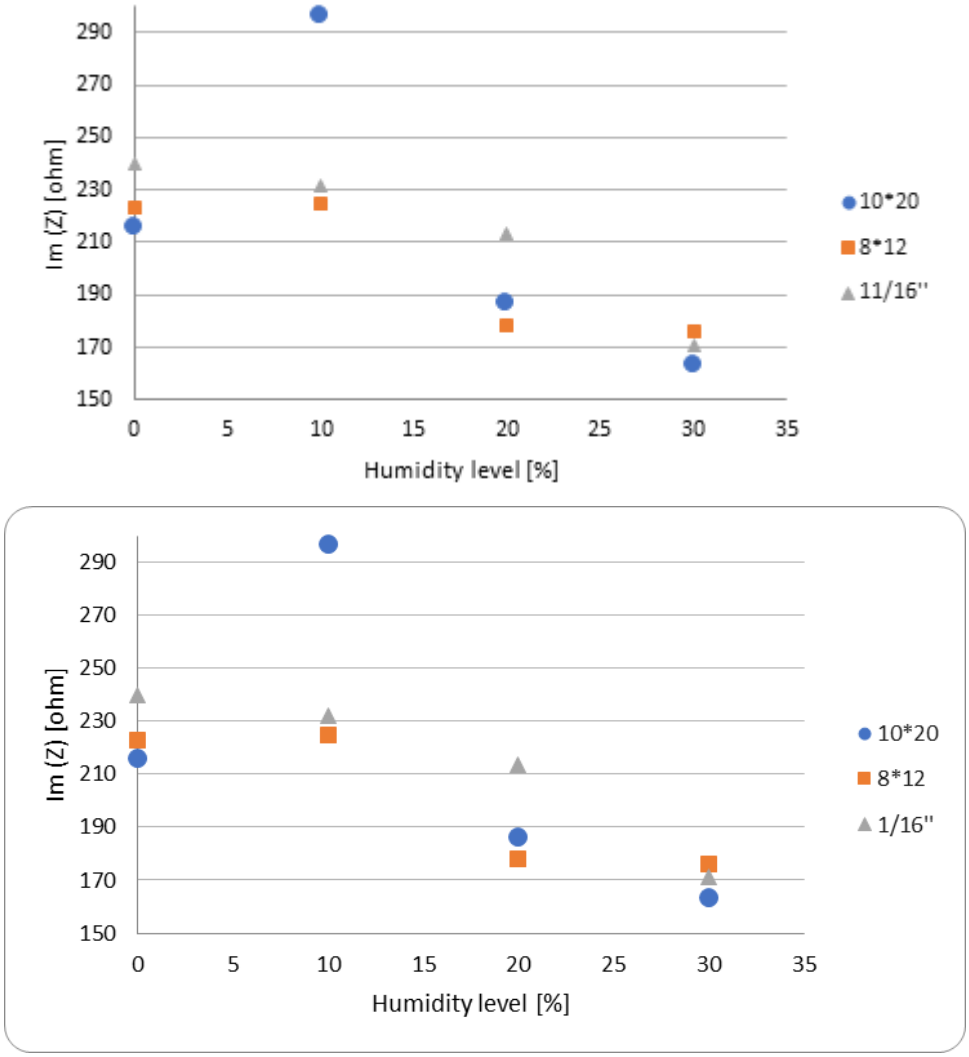

Figure 14: imaginary part of impedance of the tested samples at different humidity levels.

In contrast, the imaginary part of the impedance showed a decreasing monotonous function relative to the humidity level. A peculiarity at 10% moisture level for the 10x20 material was again evident.
The impedance values measured for all the 3 material samples are promising for the radio frequency heating process.
The values obtained will be used for the modelling activities within WP2 and WP3.

8.4. RF heating

Regarding the RF heating, the different materials were placed in a cylindrical metal container with an on-house planar circular electrode to provide the RF power. The material and electrode were positioned inside a Faraday cage for safety reasons.
With the purpose of verifying the proper heating by RF method, the material was exposed to 200 W RF power at a frequency of 27.12 kHz to reach approximately 200°C (starting from ambient temperature, approximately 20°C).
The temperature was measured using two methods: thermal imaging and optic fibers. Thermal imaging provided information about the average surface temperature of the

material, while the optic fibers measured the temperature inside the material, but just in few points. For the thermal images a FLIR thermal camera (Instrument 2) was used.

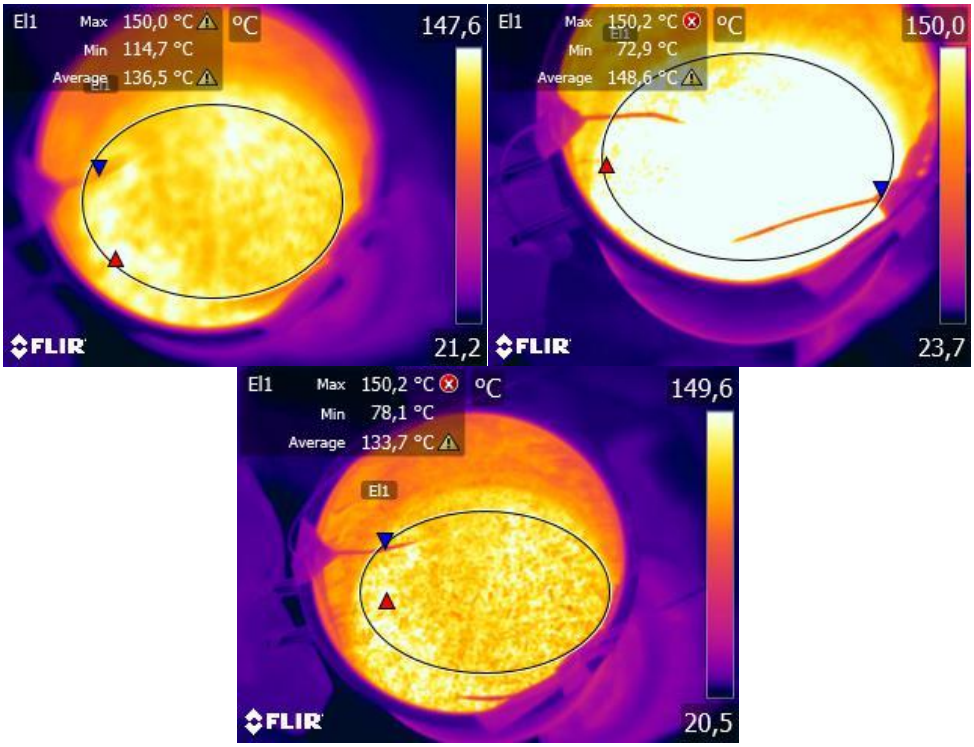

Figure 15: Thermography of 13x 1/16''

As can be seen from the pictures, the heat distribution is quite uniform in the surface. The thermal images were analysed with the camera software to get the mean temperature values for the 3 samples, reported in Table 6.

Table 6: mean temperature of the samples during the IR camera test.

Name	Size	Weight [g]	Power [W]	T [°C]	Mean [°C]
13xp	10*20	238.67	200	221.1	136.5
13xp	8*12	237.43	200	220.3	148.6
13x (pellets)	1/16''	233.48	200	225.1	133.7

Regarding the internal temperature of the material given by the optic fibres (Instrument 6), 200°C were reached after approximately 7 minutes for the spherical materials (13xp), while for the pellets the temperature was reached in about 6 minutes. The use of the optic fibres is required because of the RF field inside the material that can affect other temperature sensors as PT100 or PT1000.

The drying process involved monitoring the internal temperature of the sample over time, as shown in the following Figure 16.

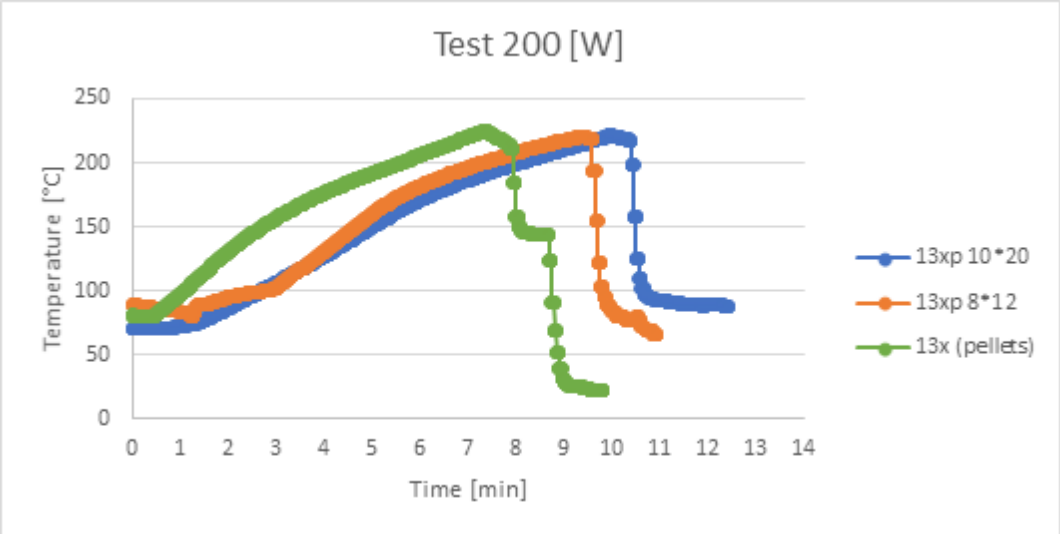

Figure 16: temporal evolution of RF-driven drying process of the samples.

The process shows that the materials respond well to radio frequency heating, especially considering the very small power amount delivered from the RF generator, in particular the cylindrical 13x 1/16'' pellet, which reaches 200°C in the shortest time. Starting from the results of these first test carried out on small samples of material and with low power, the result can be generalized, and the specific power needed to get a 150°C temperature increase in the material, in a time of 6-7minutes, is shown in Table 7.

Table 7: specific energy for the charging process on the three selected samples.

Type	[min]	Energy per kilo [Wh/kg]
10*20	9.83	137.29
8*12	8.16	114.56
1/16''	7	99.94

9. Numerical simulation of the selected materials and sensitivity analysis during discharging conditions

9.1. Model description

In order to complete the preliminary analysis on the selected TCM material, a 2D - numerical model for a small portion of a TES system was implemented in COMSOL Multiphysics® 6.1 to investigate heat and mass transfer processes during the discharge operation of the heat storage process.

The simulated geometry (**Figure 17**) is a bed filled with pellets of zeolite 13X cooled by water flowing within a heat exchanger (HEX) to ensure the water vapour adsorption. The thermochemical system was assumed a porous medium and modelled as a pseudo-homogeneous continuum elementary volume representative both of sorbate and sorbent. Heat transfer in porous medium, mass transfer in porous medium, and Darcy's law interfaces were used to model the physical-chemical processes taking place. The heat transfer interface was used to model the convection-diffusion in the porous matrix and the convection within the heat exchanger, the mass transfer interface to model the temporal variation of the concentration of water vapor transported through the zeolite 13x, and Darcy's law interface to model the flow of the water vapor into the porous matrix.

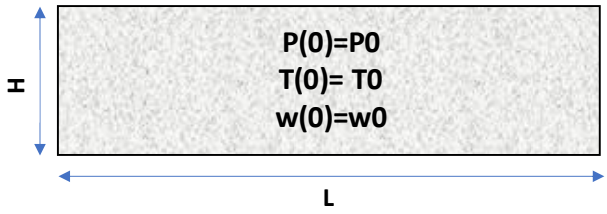

(a) Initial conditions

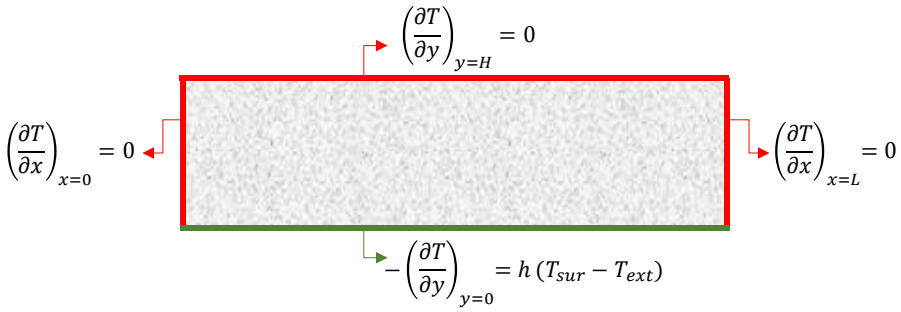

(b) Heat transfer process

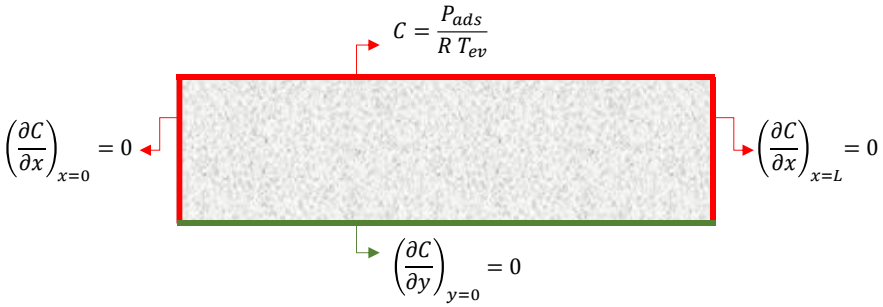

(c) Mass transfer process

***Figure 17**: Computational domain, initial and boundary conditions assumed in the simulations.*

9.1.1 Assumptions and boundary conditions

Based on either experimental evidence or previous studies the following assumptions were made:

- Zeolite 13X is a homogeneous and isotropic porous medium;
- Water vapor is assumed to be an ideal gas;
- Gas phase is in thermal equilibrium with the solid phase;
- Diffusion of heat and vapor are the only physical processes taking place;
- The diffusivity coefficient is temperature independent;
- Radiative heat losses to the ambient are neglected;
- The heat and reaction rate owing to the sorption process is modelled as volumetric sources;
- The system is initialised at the adsorption pressure P0 and regeneration sorbent temperature T0;
- The initial equilibrium concentration C0 is calculated at P0 and T0;
- The adsorption heat is supplied to the final user at the adsorption temperature Tads of 35°C;
- Evaporation heat is provided at the evaporator temperature Tev of 25°C;
- The heat exchanger (HEX) is simulated through a proper boundary condition;
- Transient simulations.

The following boundary conditions (Figure 17b) were assumed for the heat transfer process:

- Convective heat flux (Neumann's condition) with the heat exchanger on the lower face
- Symmetry on the upper face.
- Symmetry on the lateral sides.

The convective heat flux q''_{con} [W/m^2] was evaluated according to Newton's law:

$$q''_{con} = h\,(T_{sur} - T_{ext}) \quad (6)$$

where h is the convective heat transfer coefficient [W/m2 K], T_{sur} the temperature of the surface in contact with the heat exchanger, and T_{ext} the temperature of the fluid

flowing into the heat exchanger. As a calibration parameter of the model h was posed 700 [W/m2 K]. T_{ext} was posed equal to the adsorption temperature 35 °C.
The following boundary conditions (Figure 17c) were assumed for the mass transfer process:

- Concentration (Dirichlet's condition) on the upper face;
- No flux on the lower face;
- Symmetry on the lateral sides.

9.1.2 Model implementation

The mathematical model describing the mass and energy transfer processes consists of algebraic and partial differential equations.
The heat transfer is dominated by the conduction that can be expressed by Fourier's law:

$$\begin{cases} \dfrac{\partial(\rho\ cp\ T)}{\partial t} - \nabla(\lambda\ \nabla T) + u \cdot \nabla\big(\ (\rho\ cp)_{vap}\ \ T\big) = q'''_{sorp} \\ \rho\ cp = (1-\varepsilon)(\rho\ cp)_{eff} + \varepsilon\ (\rho\ cp)_{vap} \\ \lambda = (1-\varepsilon)\lambda_{eff} + \varepsilon\ \lambda_{vap} \end{cases} \quad (7)$$

Where T is the temperature [K], ρ the density [kg/m^3], cp the specific heat capacity [J/(kg K)], λ the thermal conductivity [W/(m K)], ε the bed porosity (0.6), q'''_{sorp} the volumetric sorption heat source [W/m^3], and u the Darcy velocity [m/s]. The effective properties (*eff*) of the sorbent layer take into account the vapor content (*vap*) in its adsorbed state and were evaluated as follows:

$$\rho_{eff} = \rho_{sor,dry} + \omega\ \rho_{vap,ads} \quad (8)$$

$$cp_{eff} = cp_{sor,dry} + \omega\ cp_{vap,ads} \quad (9)$$

$$\lambda_{eff} = \lambda_{sor,dry} + \omega\ \lambda_{vap,ads} \quad (10)$$

where the subscripts *sor, dry,* and *vap, ads* stand for dry sorbent and adsorbed vapor, respectively.
Water vapor thermodynamic properties were assumed temperature dependent [15] while for the dry zeolite 13X, 800 [kg/m^3], 0.88 [kJ/(kg K)],0.4 [W/(m K)] were imposed for density, specific heat capacity, and thermal conductivity, respectively [16,17].
The volumetric heat source was evaluated as function of the adsorption rate $\frac{d\omega}{dt}$:

$$q'''_{sorp} = (1-\varepsilon)\ \Delta H_{ads}\ \rho_{eff}\ \frac{\partial w}{\partial t} \quad (11)$$

where ΔH_{ads} is the adsorption enthalpy [J/kg] given by the sum of the Dubinin potential A and the latent heat of vaporization H_{ev} of the pure sorbate:

$$\Delta H_{ads} = A + H_{ev} \quad (12)$$

The loading capacity and the adsorption potential were evaluated as follows:

$$\begin{cases} w = w_0 \exp\left(-\left(\frac{A}{E}\right)^n\right) \\ A = R_{vap}\, T\, ln\left(\frac{P_{sat}}{P}\right) \end{cases} \quad (13)$$

Where w_0 is the maximum adsorption capacity [g/g], E the characteristic energy associated with the working pair [J/kg], n the surface heterogeneity parameter, R_{vap} [J/kg K] the water vapor gas constant, P and P_{sat} the adsorption and saturation pressure [Pa], respectively. By fitting the experimental dynamic sorption vapor data, the following values were found: $w_0 = 0.29$ [g/g], E=869552 [J/kg], n=1.558.
The flow axial velocity of the vapor in the porous domain was evaluated by Darcy's law:

$$\begin{cases} \varepsilon \frac{\partial \rho}{\partial t} + \nabla(\rho\, u) = 0 \\ u = -\frac{k}{\mu_{vap}} \nabla p \end{cases} \quad (14)$$

where μ is the dynamic viscosity [Pa s and k the permeability evaluated with the Kozeny-Carman approach as function of the average particle diameter d [m]:
The mass balance inside the domain can been expressed as follows:

$$\varepsilon \frac{\partial c}{\partial t} + \frac{\partial(\rho_{vap}\, cp_{\,vap})}{\partial t} - \nabla\left(D_{eff} \nabla c\right) + u \cdot \nabla c = R''' \quad (15)$$

where c is the vapor concentration [mol/m^3], D_{eff} the effective diffusion coefficient, and R''' the volumetric reaction rate [mol/m^{3}s] expressed as follows:

$$R''' = -\frac{1}{\varepsilon_p} \frac{\rho_{sor}}{M_{vap}} \frac{d\omega}{dt} \quad (16)$$

where ε_p is the particle porosity (0.4) , and $M_{\,vap}$ the molecular weight of water [kg/mol].

9.2. Main results

9.2.1 Model validation

The numerical model was validated against the experimental data discussed in Saylgan et al. (2016). As depicted in Figure 18 the simulation results showed good agreement with the experimental data of water vapor adsorption on zeolite 13X at 35 °C and 2000 Pa.

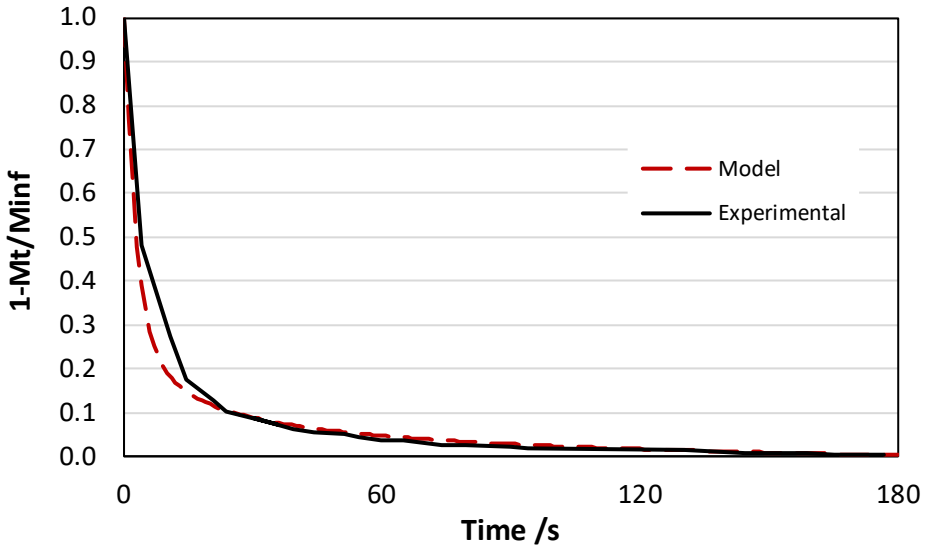

***Figure 18**: Comparison of experimental and simulated data for water-zeolite 13x.*

The data were compared in terms of the instantaneous difference in mass relative to the infinite condition:

$$1 - \frac{M(t)}{Minf} = 1 - \frac{w(t) - w(0)}{winf - w(0)} \quad (17)$$

No significant deviations confirm that the model can accurately reproduce the experiments carried out and represents a good sizing tool.

9.2.2 Sensitivity analysis

Once validated the model was used to perform a parametric analysis aiming at investigating the effect of adsorption temperature Tads and adsorption pressure Pads on the storage performance of a reactor 30 cm high and 10cm wide. The results were compared in terms of storage efficiency η_{ads} defined as follows:

$$\eta_{ads} = \frac{Q_f}{q'''_{sorp}} \quad (18)$$

where Q_f is the thermal power transferred to the thermal fluid flowing into the heat exchanger and, q'''_{sorp} the thermal power that is possible to extract from the 13X during the discharge eq (11).

Figure 19 shows the temporal trend of the adsorption uptake at adsorption pressure of 2000Pa for three values of the adsorption temperature (from 30 to 40 °C). The increase in temperature implies a decrease in the quantity of vapour adsorbed and, as a consequence, in the stored energy. This result could be explained considering that the increase in temperature hinders the available sites to absorb vapour due to the thermal agitation of the molecules adsorbed to the surface gaseous state. η_{ads} and q'''_{sorp} decreased from 49.89% to 49.52% and from 159.73 Wh/kgzeo to 149.05 Wh/kgzeo, respectively, when Tads increased from 30 °C to 40 °C. As shown in Table 8, reporting the time to reach the 80% of the maximum uptake ($\tau_{0.8}$), the higher the temperature, the higher the time of adsorption.

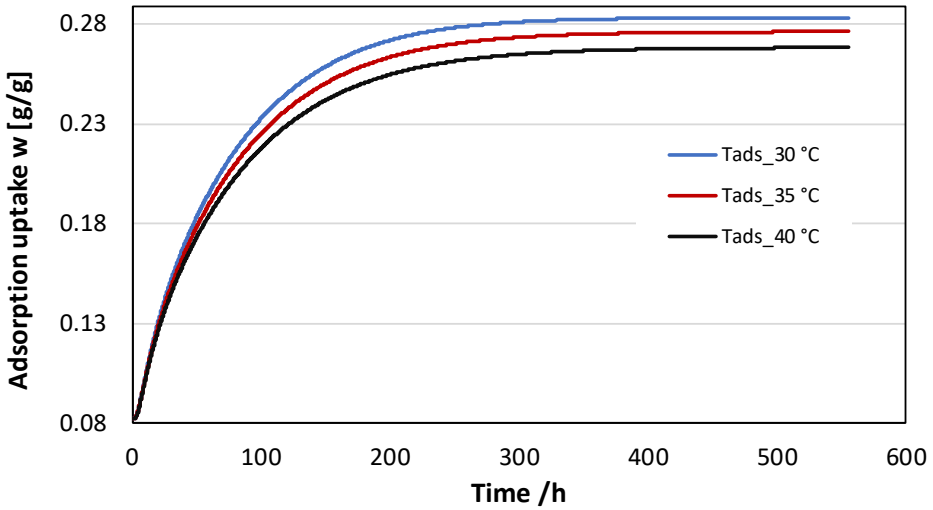

***Figure 19**: Effect of the adsorption temperature on the discharge performance of the reactor (Pads=2000 Pa).*

Table 8: Effect of the adsorption temperature on the discharge time of the reactor.

	Tads_30 °C	**Tads_35 °C**	**Tads_40 °C**
w_{max} [g/g]	0.279	0.272	0.264
$W_{0.8}$ [g/g]	0.224	0.218	0.211
$\tau_{0.8}$ [h]	92.39	94.61	95.89

Figure 20 shows the temporal trend of the adsorption uptake at the adsorption temperature of 35°C for three values of the adsorption pressure (from 1500 to 2500 Pa). In contrast to what observed in Figure 19, the higher the pressure, the higher the quantity of vapour adsorbed. η_{ads} and q'''_{sorp} enhanced from 49.33% to 50.12% and from 151.93 Wh/kgzeo to 155.51 Wh/kgzeo, when pads increased from 1500 Pa to 2500 Pa. As shown in Figure 20,the higher the pressure, the lower the time of adsorption.

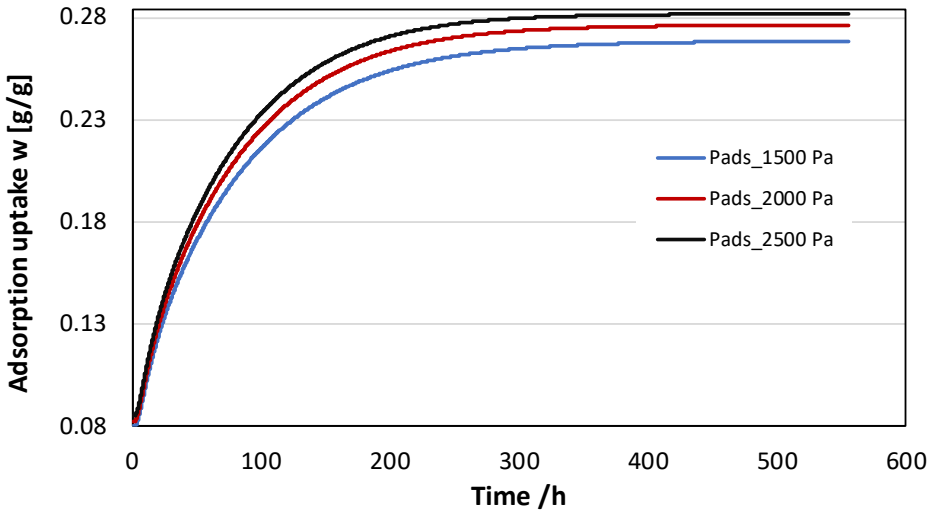

***Figure 20**: Effect of the adsorption pressure on the discharge performance of the reactor (Tads= 35°C).*

Table 9: Effect of the adsorption pressure on the discharge time of the reactor.

	Pads_1500 Pa	**Pads_2000 Pa**	**Pads_2500 Pa**
w_{max} [g/g]	0.264	0.272	0.278
$W_{0.8}$ [g/g]	0.212	0.218	0.222
$\tau_{0.8}$ [h]	98.83	94.61	90.39

The results here presented can be useful for a first analysis of the heat exchanger, which represents the core component to be designed for the discharging process. From this analysis, it is possible to notice, as first result, that a HEX with a max distance between the tube and the storage material of 30 cm, still exhibits a reasonable adsorption time. This goes into the direction indicated in the Grant Agreement, i.e., the use of a small HEX to cover discharge power, in contact with a small amount of material. This allows for a significant cost reduction compared to the state of art thermochemical HEXs.

10. Conclusions

The present deliverable has reported the selection process for the storage material in HYSTORE TCM solution. To this aim, experimental data on different materials were used and a systematic approach based on a ranking process was applied. As a result, 13X zeolite produced in Italy in large batches by UOP was selected, which also minimises risks due to availability and supply chain disruptions. A full characterization is presented, which includes adsorption properties, specific heat (carried out at CNR) and specific energy for charge with radiofrequency (carried out at INOVA with the support from SOR). Finally, discharging characterization of the material was carried out using a numerical model, which was validated against literature data.
The results will be used for a more detailed design of the TCM HYSTORE components and overall system in the subsequent activities in WP2 and WP3.

OUR TEAM

See you online!

"Funded by the European Union. Views and opinions expressed are however those of the author(s) only and do not necessarily reflect those of the European Union or European Climate, Infrastructure and Environment Executive Agency (CINEA). Neither the European Union nor the granting authority can be held responsible for them."